Performance comparison of iterative algorithms for generating digital correlation holograms used in optical security systems

David Abookasis, Amit Batikoff, Hagay Famini, and Joseph Rosen

An optical security system based on a correlation between two separate binary computer-generated holograms has been developed and experimentally tested. The two holograms are designed using two different iterative algorithms: the projection-onto constrained sets algorithm and the direct binary search (DBS) algorithm. By placing the ready-to-use holograms on a modified joint transform correlator input plane, an output image is constructed as a result of a spatial correlation between the two functions coded by the holograms. Both simulation and experimental results are presented to demonstrate the system's performance. While we concentrate mainly on the DBS algorithm, we also compare the performance of both algorithms.

OCIS codes: 070.4560, 070.2590, 090.1760, 100.4550, 100.3010.

1. Introduction

Information security techniques using optical means have received increasing attention because of their inherent parallelism, high processing speed in real-time applications, and the obstacles they present to impostors. The goal of these techniques is to conceal information such as annotations, seals, or identification numbers within a host data set. The information is hidden such that the message cannot be read by unauthorized persons. Most of the security techniques entail the use of a secret key that embeds and extracts the hidden information.[1–3]

We recently proposed and demonstrated an optical security technique that as a result of a spatial correlation between two separated computer-generated holograms (CGHs) yields a desired image.[4] We call this technique a digital correlation hologram (DCH). For security applications, one of the holograms is used as a general verification lock function designed to recover, one at a time, different hidden information from many other authorized holograms.

The authors are with the Department of Electrical and Computer Engineering, Ben-Gurion University of the Negev, P.O. Box 653, Beer-Sheva 84105, Israel. J. Rosen's e-mail address is rosen@ee.bgu.ac.il.

Received 24 August 2005; revised 30 November 2005; accepted 21 December 2005; posted 4 January 2006 (Doc. ID 64233).

0003-6935/06/194617-08$15.00/0

The synthesis process of the DCH has been based on the projection-onto constrained sets (POCS) algorithm. In this scheme a double random phase function is transformed back and forth between two domains in a joint transform correlator (JTC) configuration.[5] Appropriate constraints are employed until the function converges such that the error between the desired and the obtained image is minimal. Finally the two-phase functions are coded into positive real transparencies as a CGH[6] in order to display them on a spatial light modulator (SLM). A cross correlation between the two coded functions yielded a meaningful image. Although the POCS algorithm is a relatively rapid iterative process, it usually reaches a suboptimal solution in the sense that the final hologram does not yield an image close enough to the desired image. Consequently, the constructed image in the system output is distorted. Therefore to assess the performance of the POCS it seems worthwhile to compare the quality of the image reconstructed from the POCS to the image reconstructed from a hologram synthesized by another algorithm. In this study we perform this comparison with the direct binary search (DBS) algorithm. The hologram generated by the DBS algorithm is near optimum as it minimizes the mean square error (MSE) between the reconstruction and the object for a given random start.[7]

The DBS is initiated by generating a random binary hologram. The sampled reconstructed image is computed, and the MSE is calculated between the desired object and the optimally scaled reconstruc-

tion. The CGH is then scanned and the pixels are inverted one by one until no inversions are retained during an entire iteration. The resulting CGH is optimum in the sense that it reconstructs an image with the almost lowest possible MSE and the almost highest possible diffraction efficiency. This basic procedure is now adjusted to JTC geometry for hiding information. Because of the computational intensiveness of the DBS algorithm that is primarily due to the fact that the MSE calculation has to be repeated for every addressable cell during each of the iteration and Fourier transform operation, this technique has been limited to the synthesis of CGHs with a relatively small number of addressable cells. Several efficient algorithms have been suggested for reducing this computational intensiveness. These efficient algorithms also aimed to increase the capability of designing a DBS with a larger number of pixels.[8–10] However, this drawback does not affect the security system since once the hologram is produced, it is placed at the input of the system that reveals the secret information in a real-time operation.

A comparison summary for generating the correlation hologram using the DBS algorithm versus the POCS algorithm is essential at this point. The POCS algorithm is divided into two stages: In the first stage we compute two complex phase functions; in the second stage, these functions are then coded as real positive transparencies. In the DBS algorithm the generation requires one stage; we work directly with the hologram and the desired image. The double random phase function in the POCS is transformed back and forth between two domains and appropriate constraints are employed until the function converges, in the sense that the error between the desired and the obtained image is minimal. In the DBS no constraints are employed and by pixel flipping, the iteration process seeks the binary CGH that minimizes the error between the reconstructed and the desired images. On the other hand, the DBS is computationally more intensive because of the many Fourier transforms and the MSE repetition for every pixel during the iterations. Therefore the DBS algorithm requires much more computational time.

To make the comparison between the two algorithms reasonable, the medium of their produced holograms must be the same. As mentioned above, the DBS yields binary holograms, whereas the POCS has originally[4] yielded multitransmission level holograms. Therefore we modify the POCS algorithm such that instead of encoding the resulting phase functions to real multilevel transmissions these phase functions are encoded to a binary mask. In other words, this study presents two new algorithms for synthesizing binary DCH and compares them. One is the DBS and the other is a modified POCS that can be considered as a binary POCS. Both algorithms produce similar holograms for the same application and therefore the comparison between them is valuable. It should be emphasized that by encoding the resulting phase functions to binary rather than to gray level masks, the information of these phase functions is by no means lost but instead it is encoded to binary-valued masks. One can understand this by an analogy to the printing world in which the gray-tone images are encoded to binary halftone images without considerable damage in picture quality.

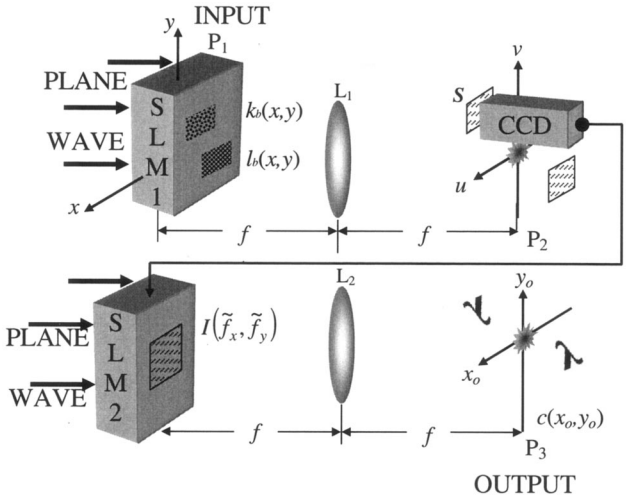

Fig. 1. Schematics of a modified JTC used for both the computer simulation and the optical experiments.

The paper is divided into five sections. Section 2 describes the construction and correlation of the subholograms using the DBS algorithm. Section 3 presents the computer simulation, and Section 4 presents the optical experimental results. Conclusions are presented in Section 5.

2. Correlation Holograms using the Direct Binary Search Algorithm

In our security technique, the POCS and the DBS algorithms are implemented by a digital procedure that is based on simulating the modified JTC depicted in Fig. 1. In this setup we mask the joint spectral plane and process only the first diffraction order in this plane. This procedure enables us to obtain the cross correlation between, effectively, two complex functions, although there are actually two real, nonnegative, binary functions in the input plane. Implementation of the POCS algorithm was described extensively in Ref. 5 and is not repeated here. Here we concentrate on implementing the DBS algorithm.

We start the DBS procedure by defining two binary subholograms positioned jointly at two different locations on the input plane. One binary hologram, the key hologram in the security scheme, $k_b(x, y)$, is initiated as a random binary mask with an equal probability to get the values 0 or 1. This hologram is changed along the DBS process in order to reduce the MSE between the reconstructed and the desired images. The initial key hologram is given by

$$k_b(x, y) = B(x, y)\mathrm{rect}\left(\frac{x}{A}, \frac{y}{B}\right) * \delta(x - a, y - b), \tag{1}$$

where $B(x, y)$ randomly gets values 0 or 1 in equal probability, the function $\mathrm{rect}(x/A, y/B)$ is defined as 1 for $|x|, |y| \le A/2, B/2$ and 0 otherwise, while A, B are the dimensions of the hologram in the x and y directions, respectively. The * denotes the convolution operation, δ is the Dirac delta function, and the key hologram is centered around the point (a, b).

The other hologram $l_b(x, y)$ is used as a security lock of the system, and as such it is determined once in the beginning of the process. This hologram is fixed during the iterative process and is not related to the first subhologram or the output image. Moreover, this same hologram can be used constantly in the system verifying authentically the infinity amount of other different-from-user-to-user holograms. To direct as much as possible light intensity into the recorded area S on plane P_2, the lock function is determined as

$$l_b(x, y) = \mathrm{Bin}\{\cos[2\pi(\alpha x + \beta y) + \phi_r(x, y)]\} \times \mathrm{rect}\left(\frac{x}{A}, \frac{y}{B}\right) * \delta(x + a, y + b), \quad (2)$$

where $\phi_r(x, y)$ is a random function uniformly distributed in the range $[-\pi, \pi]$, and (α, β) are the spatial carrier frequencies that direct the light to area S. The function $\mathrm{Bin}\{a\}$ is defined as 1 if $a > 0$ and 0 otherwise.

After the two holograms have been constructed, the modified JTC path iteration is begun. The reconstructed image is computed in plane P_3, and the MSE is calculated between the desired image and the obtained reconstruction in the nth iteration. $k_b(x, y)$ is then scanned and the pixel values are inverted one by one to a complementary binary value. After each inversion the MSE is calculated again through the modified JTC path. If the error has decreased, the inverted pixel is retained and the next pixel is inverted. Otherwise, the inverted pixel is restored to its previous value before proceeding to the next pixel. One iteration of the algorithm consists of a single trial inversion of every pixel in $k_b(x, y)$. The search process is terminated when within a single iteration no pixels are found to produce a decrease in the reconstruction error. The resulting hologram is optimum in the sense that it reconstructs an image with the lowest possible MSE. Note that, although the process of the modified JTC includes two Fourier transforms, the first transform can be avoided since the effect of flipping one binary value of $k_b(x, y)$ is equivalent to adding (in case of flipping from 0 to 1) or to subtracting (in case of flipping from 1 to 0) a linear phase function to, or from, the spatial spectrum at plane P_2, with a frequency determined by the location of the flipped pixel.

As depicted in Fig. 1, the two binary holograms $k_b(x, y)$ and $l_b(x, y)$ are now displayed around the points $(\pm a, \pm b)$ on input plane P_1 of the modified JTC, on SLM1, and are jointly Fourier transformed onto plane P_2 by lens L_1. Only part of the joint transform power spectrum is observed on plane P_2 of the modified JTC. This area designated as S is centered around the point (α, β) and has the size of $\widetilde{A} \times \widetilde{B}$ pixels. The complex amplitude on plane P_2 inside area S is

$$\begin{aligned} H(f_x, f_y) &= \Im_{2D}\{k_b(x, y) + l_b(x, y)\}\mathrm{rect}\left(\frac{f_x - \alpha}{\widetilde{A}}, \frac{f_y - \beta}{\widetilde{B}}\right) \\ &= K(f_x - \alpha, f_y - \beta)\exp[-i2\pi\{(f_x - \alpha)a \\ &\quad + (f_y - \beta)b\}] + L(f_x - \alpha, f_y - \beta) \\ &\quad \times \exp[i2\pi\{(f_x - \alpha)a + (f_y - \beta)b\}], \end{aligned} \quad (3)$$

where $\Im_{2D}$ is two-dimensional Fourier transform, and $K(f_x, f_y)$ and $L(f_x, f_y)$ are part of the Fourier transform of $k_b(x, y)$ and $l_b(x, y)$, respectively, inside rectangle S. $(f_x, f_y) = (u/\lambda f, v/\lambda f)$, (u, v) are the spatial coordinates of plane P_2, λ is the wavelength of the illuminated plane wave, and f is the focal length of lens L_1. The CCD camera is positioned at the back focal plane of the first lens and catches only part of the power spectrum inside area S. The intensity distribution recorded by the CCD is therefore

$$\begin{aligned} I(\tilde{f}_x, \tilde{f}_y) &= \left|\exp\left[-i2\pi\left(a\tilde{f}_x + b\tilde{f}_y\right)\right]K(\tilde{f}_x, \tilde{f}_y) \right. \\ &\quad \left. + \exp\left[i2\pi\left(a\tilde{f}_x + b\tilde{f}_y\right)\right]L(\tilde{f}_x, \tilde{f}_y)\right|^2 \\ &= \left|K(\tilde{f}_x, \tilde{f}_y)\right|^2 + \left|L(\tilde{f}_x, \tilde{f}_y)\right|^2 \\ &\quad + \exp\left[-i4\pi\left(a\tilde{f}_x + b\tilde{f}_y\right)\right]K(\tilde{f}_x, \tilde{f}_y)L^*(\tilde{f}_x, \tilde{f}_y) \\ &\quad + \exp\left[i4\pi\left(a\tilde{f}_x + b\tilde{f}_y\right)\right]K^*(\tilde{f}_x, \tilde{f}_y)L(\tilde{f}_x, \tilde{f}_y), \end{aligned} \quad (4)$$

where $(\tilde{f}_x, \tilde{f}_y) = (f_x - \alpha, f_y - \beta)$ are spatial frequency coordinates of the camera and the upper asterisk denotes complex conjugation.

The intensity pattern of Eq. (4) is then displayed on the second SLM denoted by SLM2 in Fig. 1. This SLM is illuminated by a plane wave such that the Fourier transform of the SLM transparency is obtained in the back focal plane P_3 of lens L_2. Assuming that the focal length of L_2 is identical to that of L_1, the Fourier transform of $I(\tilde{f}_x, \tilde{f}_y)$ is

$$\begin{aligned} c(x_o, y_o) &= k(x_o, y_o) \otimes k(x_o, y_o) + l(x_o, y_o) \otimes l(x_o, y_o) \\ &\quad + [k(x_o, y_o) \otimes l(x_o, y_o)] * \delta(x_o - 2a, \\ &\quad y_o - 2b) + [l(x_o, y_o) \otimes k(x_o, y_o)] * \delta \\ &\quad \times (x_o + 2a, y_o + 2b), \end{aligned} \quad (5)$$

where $k(x, y)$ and $l(x, y)$ are inverse Fourier transforms of $K(f_x, f_y)$ and $L(f_x, f_y)$, respectively. $\otimes$ denotes the correlation operation, and (x_o, y_o) are the coordinates of output plane P_3. In Eq. (5) the first two terms represent the zero-order diffraction at the origin of the output plane while the last terms represent the cross correlation between the two complex functions $k(x, y)$ and $l(x, y)$ around points $(x_o = 2a, y_o = 2b)$ and $(x_o = -2a, y_o = -2b)$, respectively. It should be noted that, due to the unique operation of the modified JTC, the resulting cross correlation is

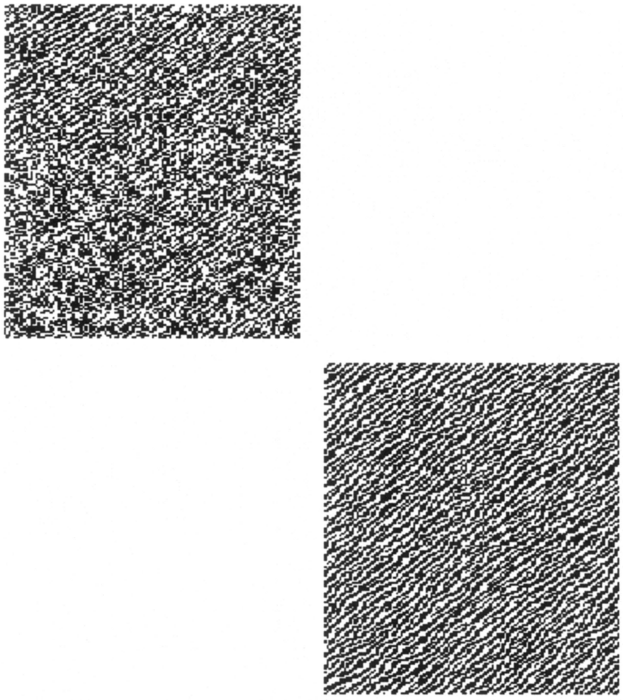

Fig. 2. Enlarged portion (550 × 550 pixels out of 1344 × 960 pixels) of the DCH transparency generated by the DBS algorithm.

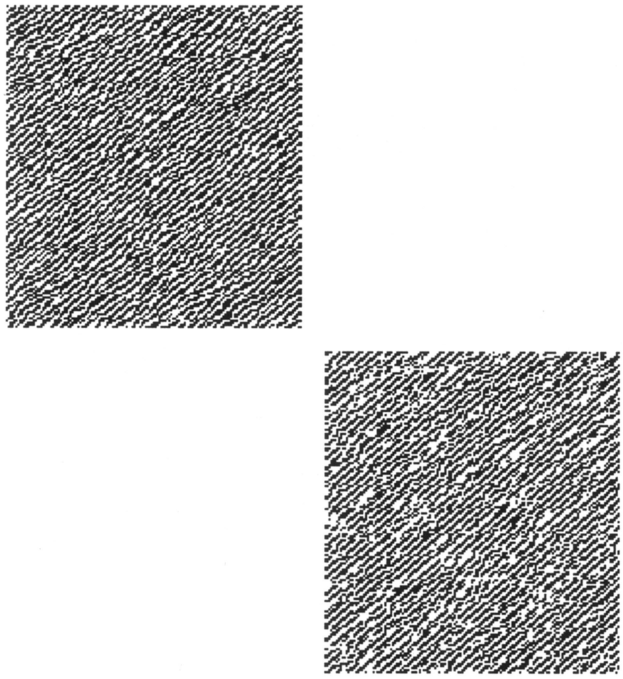

Fig. 3. Enlarged portion (550 × 550 pixels out of 1344 × 960 pixels) of the DCH transparency generated by the POCS algorithm.

between two complex functions $k(x, y)$ and $l(x, y)$, although in the input there are two binary functions $k_b(x, y)$ and $l_b(x, y)$. $k(x, y)$ and $l(x, y)$ are complex functions distributed almost uniformly on the complex plane, because each are, in general, an inverse Fourier transform of a nonsymmetric function that does not have a distinguishable pick value in its center. This feature of the modified JTC is essential, since in general one cannot get any desired image from a cross correlation between two real nonnegative functions. According to the output results of the DBS algorithm, these cross correlations approximately produce the desired image. Therefore we can retrieve the coded image by reading it from the vicinity of point $(2a, 2b)$ or $(-2a, -2b)$.

3. Simulation Results

The systems performance was demonstrated first by a computer simulation and then by an optical experiment. The purpose of the computer simulation was to evaluate the potential quality of the image constructed by our method in view of the low quality of the SLM transparencies used in the optical experiment.

In the simulation both the DBS and the POCS algorithms were tested with the same binary output image. For a fair comparison the POCS was adapted to binary data. In the end of the POCS algorithm described in Ref. 4, the two phase functions are coded as a binary CGH by setting to 1 any value of the real part that is above 0 and setting to 0 otherwise. Both subholograms were generated with 168 × 120 pixels and their cross correlation closely reconstructs the intensity distribution pattern of the Greek letter λ in a 42 × 30 pixel window.

After completing the iterations of each algorithm, both subholograms were placed in the input domain P_1 on a new matrix with a dimension of 1344 × 960 pixels. The enlarged portion of this matrix is shown in Fig. 2 for the DBS, and is shown in Fig. 3 for the binary POCS. As mentioned earlier, the DBS algorithm is computationally demanding especially for moderate- and large-sized holograms. Therefore, in order to accelerate the convergence of the algorithm and consequently reduce the computation time, we adopted a fast DBS algorithm as suggested by Chhetri *et al.*[10] The advantage of this acceleration technique is that it identifies those pixels that do not produce a reduction in the MSE before any iteration by associating each pixel with a flag indicating whether it will contribute to a reduction in the MSE in further iterations. In a particular iteration like the conventional DBS, the decision to flip the pixel depends on a probability function. Generating the holograms using this acceleration method took 36 h instead of several days. In contrast, the average CPU time required for completing the binary POCS iteration was approximately 17 s.

The convergence of the DBS and the binary POCS algorithms are shown in Fig. 4. The error values start with 3.8508×10^4 for the DBS and 0.202 for the POCS. In the DBS algorithms the iteration is stopped automatically after 18 iterations, where there are no inversions during an entire iteration. Conversely, in the POCS algorithm the iterations were stopped arbitrarily after 100 iterations. The fraction of the ad-

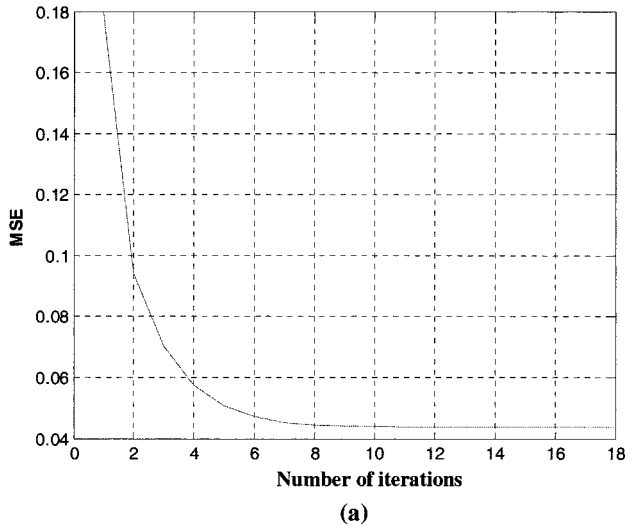

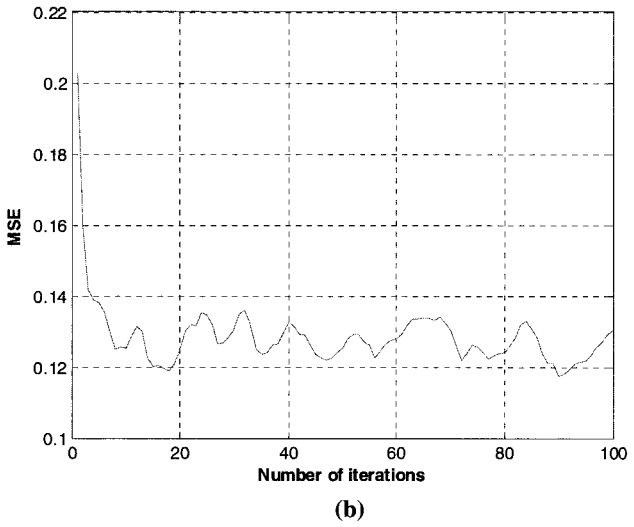

Fig. 4. MSE versus the number of iterations of the (a) DBS and (b) POCS algorithms.

dressable hologram points that changed during iteration in the case of the DBS algorithm is shown in Fig. 5. Initially, this fraction is quite large but it decreases nearly monotonically with each iteration.

As Figs. 2 and 3 show, both subholograms were placed in a diagonal position in order to escape from a large zero-order diffraction occurring at the origin of output plane P_3. Both functions from Fig. 2 (or Fig. 3) were jointly Fourier transformed to the power spectrum plane P_2. In Fig. 6 two diffraction orders of the spectral plane on either side of the zero order diffraction can be clearly seen. Since only one of these orders is needed, we output only the intensity distribution, which is denoted by the white striped line in each figure. This intensity frame was then Fourier transformed. The three orders of the correlation plane, denoted by P_3 in Fig. 1, containing our code λ in the two first diffraction orders, can be clearly seen in Fig. 7. In the case of the DBS algorithm [Fig. 7(a)], the noise is relatively low in the region where the

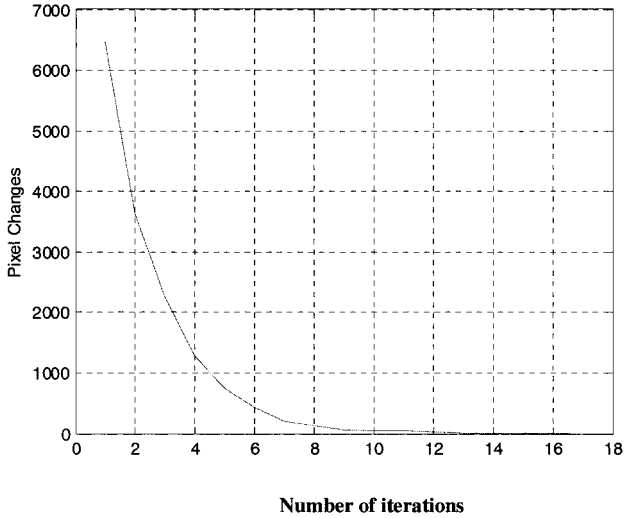

Fig. 5. Hologram pixel changes versus number of iterations during the DBS algorithm.

image is located. In comparison to the reconstruction of the binary POCS algorithm [Fig. 7(b)], the reconstruction in Fig. 7(a) is much better.

We assessed the reconstruction quality according to three different parameters: the MSE criterion, the diffraction efficiency, and our subjective visual impression. In this study we adopt the MSE as given in Ref. 7 [p. 2792, Eq. (21)]. The error was found to be 0.0438 for the DBS algorithm and approximately 0.1894 for the POCS after binarization. The minimum error for the POCS before binarization, in the case of two complex holographic functions, is 0.1175 obtained at the 90th iteration [see Fig. 4(b)]. A measure for the diffraction efficiency was also defined according to Ref. 7 [p. 2790, Eq. (14)]. For the DBS hologram the efficiency was 0.15, while for the binary POCS hologram the efficiency was only 0.0486. Comparing the visual quality of Fig. 7(a) with that of Fig. 7(b), one can be impressed that the reconstructed image of Fig. 7(a) is clearer, indicating the superiority of the DBS algorithm.

The performance of the DBS and the POCS algorithms are summarized in Table 1. From the results of this table, it can be seen that the DBS algorithms have lower reconstruction errors and higher diffraction efficiencies than the CGHs designed by the binary POCS algorithm. However, the computational time of the DBS is significantly longer.

4. Experimental Results

The experimental test was performed with the correlation system shown in Fig. 1. In the first experiments, the DBS hologram (Fig. 2) was displayed on SLM1 (CRL, Model XGA3) and was illuminated by a 5 mW collimated beam emerging from a He–Ne laser at 632.8 nm. The complete diffraction pattern of the joint transform power spectrum behind the back focal plane of L_1 (f = 150 mm) is shown in Fig. 8(a). In these experiments, an 8-bit 795 × 596 pixels CCD

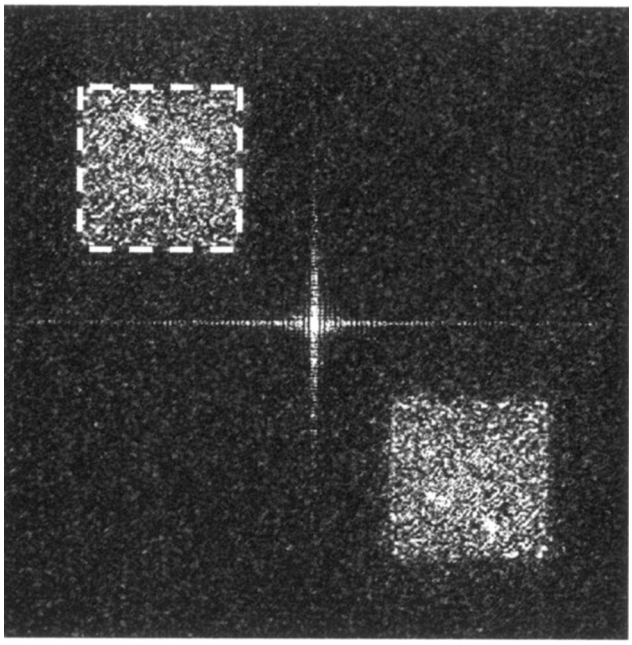

(a)

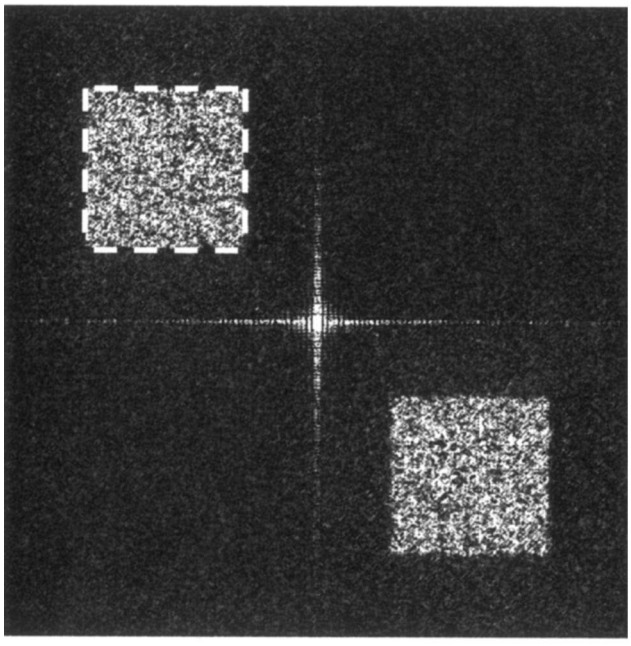

(b)

Fig. 6. Digital reconstitution of the distribution of the three diffraction orders on the power spectrum plane obtained from (a) the hologram shown in Fig. 2 and (b) the hologram shown in Fig. 3.

camera (Sony-XC75CE) was used to capture the pictures.

As in the simulation, three different orders of the diffracted wavefront on either diagonal side of the zero order can be observed in Fig. 8(a). Since only one of these orders is needed, we recorded only the intensity distribution denoted by the dashed marked frame in the figure. This spectrum was then displayed on SLM2. Finally, after transforming the spectrum by

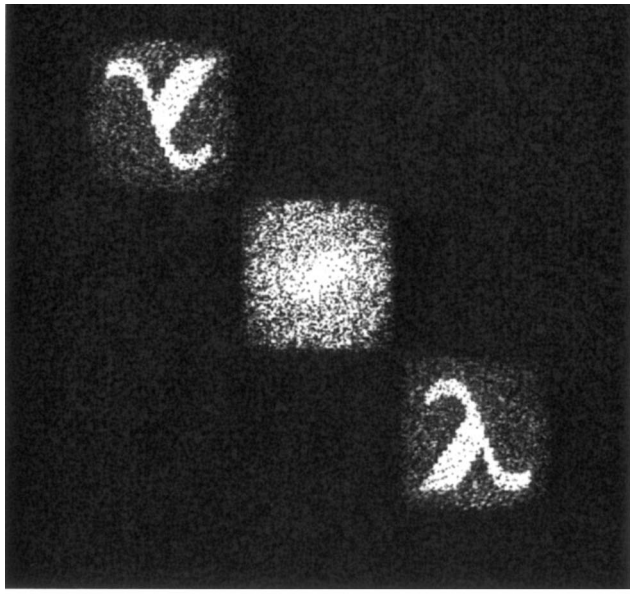

(a)

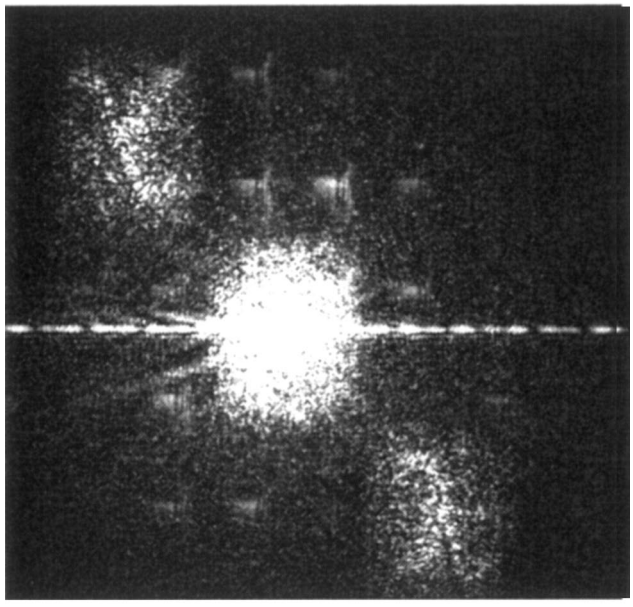

(b)

Fig. 7. Digital image reconstruction of the modified JTC output plane from Fig. 6; (a) DBS and (b) binary POCS.

lens L_2 ($f = 400$ mm), the correlation plane was obtained. Figure 8(b) depicts the hidden image reconstructed from the cross correlation between two input holograms. The three orders of the correlation plane

Table 1. Comparison Performance for DBS and Binary POCS Algorithms

Parameter	DBS	Binary POCS
MSE	0.0438	0.1894
Diffraction efficiency	0.15	0.0486
Computation time	36 h	17.265 s

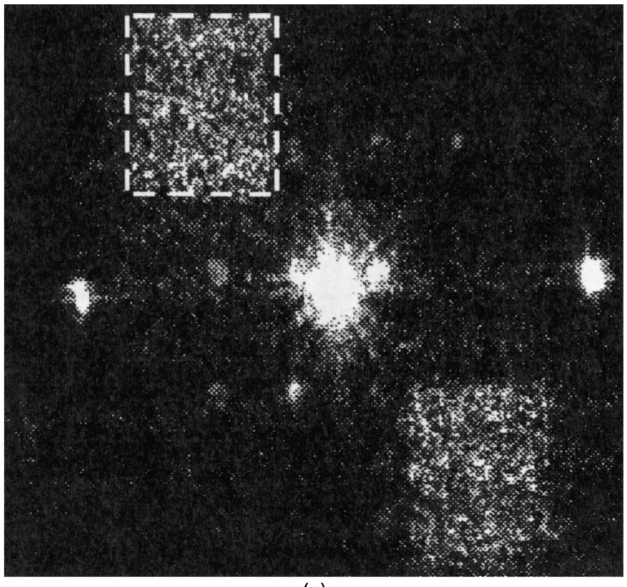

(a)

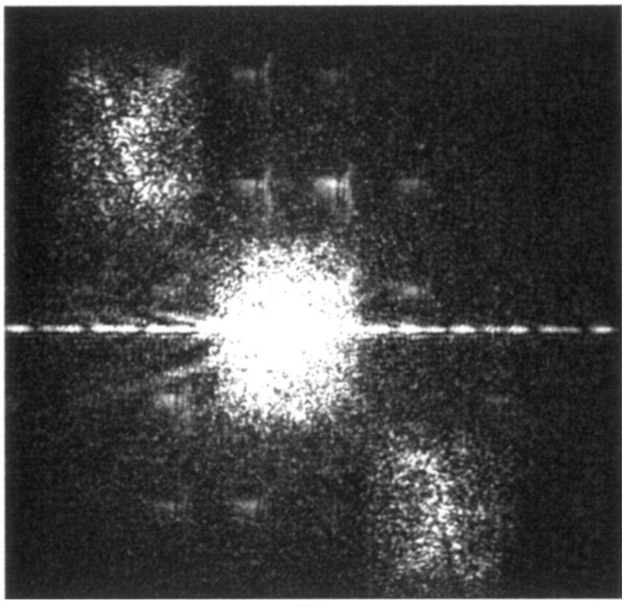

(b)

Fig. 8. DBS optical results of the (a) three diffraction orders on the power spectrum plane and (b) image construction on the correlation plane.

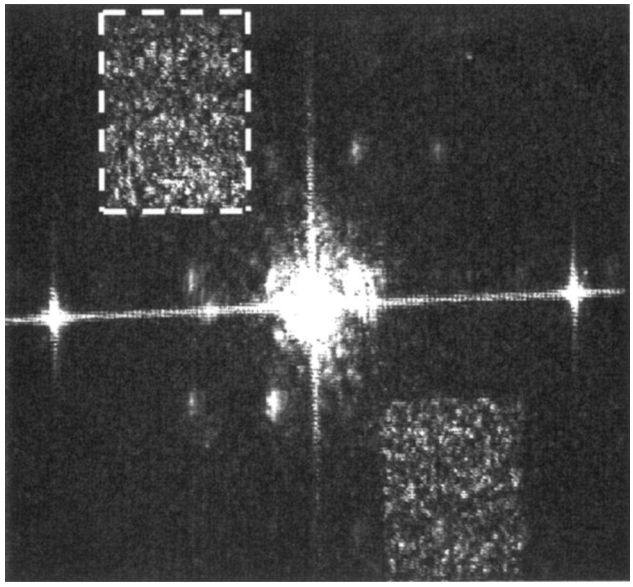

(a)

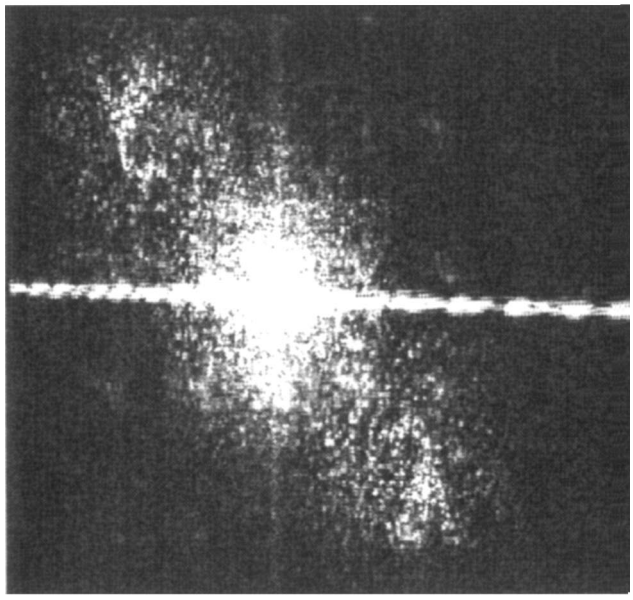

(b)

Fig. 9. Binary POCS optical results of the (a) three diffraction orders on the power spectrum plane and (b) image construction on the correlation plane.

and the image sign λ in the two first diffraction orders can be seen with less quality than the simulation results. We attribute the reduction of the image clarity between simulations and experiments to the poor quality and low resolution of the SLM. Note that between input and output a SLM is used twice in the input and the spectral planes. Therefore the level of noise and distortions are higher than in the case of reconstruction of a conventional CGH displayed on a single SLM.

The above experiment was repeated for the binary POCS hologram (Fig. 3). The complete diffraction pattern of the power spectrum behind the first Fourier lens (f = 150 mm) is shown in Fig. 9(a). As previously, we recorded only one of the intensity distributions (denoted by the dashed line) and displayed it on the second SLM (SLM2). The reconstruction results behind the Fourier lens L_2 (f = 400 mm) are shown in Fig. 9(b). The difference between the two algorithms in the optical experiments is less considerable than the difference between them in the simulations.

5. Conclusions

In this study we have proposed and demonstrated a method to implement an optical security system

based on computer-generated correlation holograms. By using two different iterative procedures, DBS and POCS, we succeeded in generating two kinds of DCH. The correlation results are constructed when this hologram is placed on a modified JTC and coherently illuminated. According to our method, one can design two holograms in order to obtain a chosen code or image. Because computation of the two holograms starts from completely random functions, they cannot be reproduced even if the output image is known. As a result, forgery becomes more difficult in comparison with other optical security systems. Despite the poor quality of the reconstructed image caused mainly by the SLM and the noise introduced by the optical elements, the DBS reconstruction was found to be superior to the binary POCS reconstruction owing to a lower MSE and higher efficiency. Simulation comparisons with experimental results verify this conclusion.

In summary, our optical security system has the advantages of simple design and alignment with a high degree of security and therefore shows promise for implementation in several practical applications. This technique can also be used for encryption systems in which the image in the correlation plane is considered as the information to be encrypted.[3,11,12]

This research was supported by Israel Science Foundation grant 119/03.

References

1. B. Javidi, "Securing information with optical technologies," Phys. Today **50**(3), 27–32 (1997).
2. H. T. Chang, W. C. Lu, and C. J. Kuo, "Multiple-phase retrieval for optical security systems by use of random-phase encoding," Appl. Opt. **41,** 4825–4834 (2002).
3. A. Sinha, and K. Singh, "A technique for image encryption using digital signature," Opt. Commun. **218,** 229–234 (2003).
4. D. Abookasis and J. Rosen, "Digital correlation holograms implemented on a joint transform correlator," Opt. Commun. **225,** 31–37 (2003).
5. D. Abookasis, O. Arazi, J. Rosen, and B. Javidi, "Security optical systems based on a joint transform correlator with significant output images," Opt. Eng. **40,** 1584–1589 (2001).
6. J. J. Burch, "A computer algorithm for the synthesis of spatial frequency filter," Proc. IEEE **55,** 599–601 (1967).
7. M. A. Seldowitz, J. P. Allebach, and D. W. Sweeney, "Synthesis of digital holograms by direct binary search," Appl. Opt. **26,** 2788–2798 (1987).
8. B. K. Jennison, J. P. Allebach, and D. W. Sweeney, "Efficient design of direct-binary-search computer generated holograms," J. Opt. Soc. A **8,** 652–660 (1991).
9. J-Y. Zhuang and O. K. Ersoy, "Fast decimation-in-frequency direct binary search algorithms for synthesis of computer-generated holograms," J. Opt. Soc. A **11,** 135–143 (1994).
10. B. B. Chhetri, S. Yang, and T. Shimomura, "Stochastic approach in the efficient design of the direct-binary-search algorithm for hologram synthesis," Appl. Opt. **39,** 5956–5964 (2000).
11. J. Ohtsubo and A. Fujimoto, "Practical image encryption and decryption by phase-coding technique for optical security systems," Appl. Opt. **41,** 4848–4855 (2002).
12. D. Abookasis, O. Montal, O. Abramson, and J. Rosen, "Watermarks encrypted in a concealogram and deciphered by a modified joint transform correlator," Appl. Opt. **44,** 3019–3023 (2005).